Resonant laser-plasma excitation of coherent THz phonons under extreme conditions of femtosecond plasma formation in a bulk of fluorine-containing crystals

2013 Laser Phys. Lett. 10 076003

(http://iopscience.iop.org/1612-202X/10/7/076003)

IOP PUBLISHING LASER PHYSICS LETTERS
Laser Phys. Lett. **10** (2013) 076003 (6pp) doi:10.1088/1612-2011/10/7/076003

LETTER

Resonant laser-plasma excitation of coherent THz phonons under extreme conditions of femtosecond plasma formation in a bulk of fluorine-containing crystals

F V Potemkin[1], E I Mareev[1], P M Mikheev[1] and N G Khodakovskij[2]

[1] Faculty of Physics and International Laser Center, Moscow State University, Moscow, 119991, Russia
[2] Prokhorov General Physics Institute, Russian Academy of Sciences, Moscow, 119991, Russia

Received 21 December 2012
Accepted for publication 2 April 2013
Published 11 June 2013
Online at stacks.iop.org/LPL/10/076003

Abstract
The dynamics of coherent phonons in fluorine-containing crystals under plasma formation were studied using a nonlinear pump–probe technique based on third harmonic generation. In LiF crystal more than one phonon mode was observed. The modes are the overtones of a fundamental wave with a frequency of 0.38 THz. In CaF_2 crystal phonons with frequencies of 1 and 0.1 THz were observed. In BaF_2 crystal, in addition to coherent phonons with frequencies of 1 THz and 67 GHz, a significant increase of amplitude in the phonon modes with a time delay of 15 ps was detected.

(Some figures may appear in colour only in the online journal)

1. Introduction

Currently, femtosecond technology is widespread, and is used for multiple applications, such as industrial manufacturing, information and communication technologies, environmental technology and life sciences (medicine, biology, chemistry) [1]. The use of ultrashort laser pulses for drilling metals is highly promising with respect to reduced melt production and recast formation, as well as minimized heat-affected zones. It enables a machining precision far superior to that achieved by longer pulses, the full potential of which, however, can frequently only be reached using low laser fluence levels at the expense of processing speed [2]. Femtosecond lasers can also be used in biology and medicine; for example, the femtosecond laser beam can be used as a tool to remove either decayed enamel/dentin—also named caries—or as a tool to remove ceramic from a bulk until the shape of an all-ceramic restoration is left. Another interesting application of femtosecond lasers in medicine is laser reshaping of cartilage [3]. Femtosecond lasers are widely used in ophthalmology, because femtosecond photodisruption opens new pathways in refractive surgery due to its precise interaction mechanism with biological tissue. Using high numerical focusing and pulse energies just above threshold for optical breakdown, disruptive effects can be generated in a range below the diffraction limit [4]. This effect can be used to cut tissue with a precision at the cellular level. This kind of cell surgery offers a new field of experimental investigation in cell biology. Femtosecond lasers are also used in stereolithography for creating various objects with complex structures, such as scaffolds [5–7]. The femtosecond laser is an important tool for attosecond pulse generation and

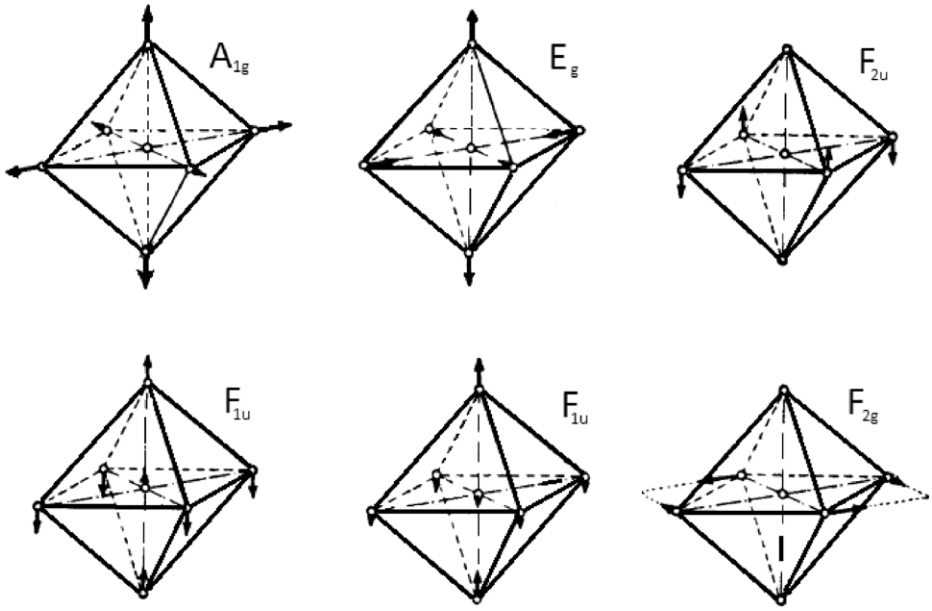

Figure 1. Examples of oscillations in crystals with O_h symmetry.

terahertz radiation [8]. Another important use of femtosecond laser radiation is micromachining. Waveguides, various active devices, filters and resonators are created using tightly focused laser radiation [9]. Tightly focused femtosecond laser radiation is also used for writing and reading 3D data [10].

The range of phenomena occurring during the interaction of tightly focused femtosecond laser radiation with dielectrics is quite wide, from multiphoton and tunneling ionization, plasma electron heating in the laser field, impact ionization and phonon excitation to shock wave propagation and residual micro-modification formation [9, 11–15]. Special attention should be paid to coherent phonon dynamics. Phonons not only give an idea of a substance's vibrational properties, but can also be used to control molecular and collective motion, to get special non-equilibrium states and to facilitate chemical and structural changes that may not occur under normal conditions [16, 17]. There are several useful models to describe coherent phonon generation. To describe the coherent phonon dynamics, the displacive mechanism (DECP), impulsive stimulated Raman scattering (ISRS) and time-dependent functional density theory are normally used [18–22].

Based on the ISRS theoretical background [23], a single ultrashort laser pulse, with spectral width greater than the intermolecular vibration frequency, can cause spatial stable collective coherent lattice vibration at the Raman active vibrational mode. The DECP theory gives the best results for the oscillations of A_{1g}, A_1 (see figure 1) symmetry excited by an ultrashort laser pulse. In equilibrium, before the pump pulse arrival, A_1 displacement is determined by the free energy minimization. When the system is excited by the pump pulse, a new equilibrium for A_1 displacements appears. The system is trying to get back to the old equilibrium position, but instead goes to A_1 coherent oscillations about the new equilibrium [24]. In [25] it was shown that stimulated Raman scattering by phonons is described by two separate tensors, one of which accounts for the phonon-induced modulation of the susceptibility, and the other one for the dependence of the coherent mode amplitude on the light intensity (DECP). These tensors have the same real component, associated with impulsive generation of phonons, but different imaginary parts. In density functional theory the kinetic energy and the energy of interaction between the parts of the system, which are functions of several variables, are replaced by functionals. These functionals depend only on the electron density of the system. Next, using numerical methods, all the parameters of the system are calculated. For coherent phonon observation the pump–probe technique is most commonly used [23].

The coherent phonon generation leads to time modulation of the third-order nonlinear medium susceptibility $\chi^{(3)}(t) = \chi_0^{(3)} + (\frac{\partial\chi^{(3)}}{\partial Q})Q(t)$, where $(\frac{\partial\chi^{(3)}}{\partial Q})$ is the Raman nonlinearity and $Q(t)$ is the the coordinate of the ion displacement relative to the equilibrium state [23]. Therefore, the efficiency of any nonlinear-optical process running on a third-order nonlinearity, such as the third harmonic generation (THG), should also be modulated in time with excitation of coherent phonons in the medium.

In our previous articles on coherent phonon studies, a modified time-resolved method of structure probing based on THG was used [26–29]. This method has proved to be successful in studies of laser plasma dynamics in fused silica samples and quartz [30], because the signal of the third harmonic is more sensitive in structure of matter changes (ionization, ion movements), as is demonstrated in [29]. Therefore, in order to study the excitation and relaxation dynamics of coherent phonons under the plasma formation regime the nonlinear-optical method based on THG was used. In the standard pump–probe scheme [23, 31] with polarization separation the channel of the third harmonic generated by the probe pulse was added [32].

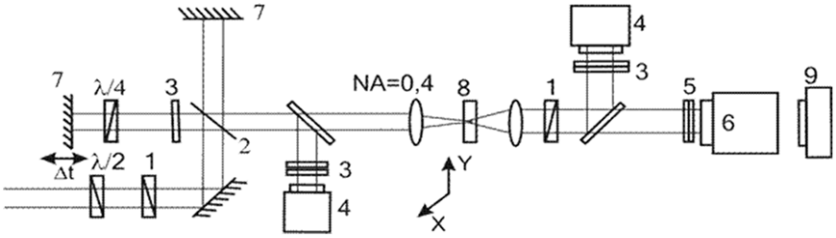

Figure 2. Experimental setup: 1 is a Glan prism, 2 is a 50/50 beam splitter, 3 are neutral filters, 4 are Ge photodetectors, 5 is a 410 ± 5 nm band-pass filter, 6 is a photomultiplier tube, 7 are silver mirrors, 8 is a sample, 9 is a CCD camera.

Table 1. Tensors of the Raman active modes for crystals belonging to the group $Fm\bar{3}m$ (a, b, c, d are constants).

A_{1g}			E_g			E_g			T_{2g}			T_{2g}			T_{2g}		
a	—	—	b	—	—	$-3^{1/2}b$	—	—	—	—	—	—	—	d	—	d	—
—	a	—	—	b	—	—	$3^{1/2}b$	—	—	—	d	—	—	—	d	—	—
—	—	a	—	—	$-2b$	—	—	—	—	d	—	d	—	—	—	—	—

In this letter the processes of excitation and relaxation of coherent phonons in fluorine-containing dielectrics such as LiF, CaF_2 and BaF_2 under the plasma formation regime are presented. In the experiments all the samples were oriented in such a way that the well-known phonon vibrations arising in the T_{2g} Raman active mode were not present in the output transmittance and third harmonic signals.

2. Experimental setup

In the experiments, radiation from a Cr:forsterite femtosecond laser system ($\lambda = 1.24$ μm, $\tau = 140$ fs, $E = 0.1$–5 μJ, intensity pulse contrast ≈ 250) was used. The use of Cr:forsterite laser radiation expands the possibilities of the pump–probe technique because its third harmonic is in the transparency region for various media. The experimental scheme is sketched in figure 1.

The half-wave plate with Glan prism 1 (see figure 2) was used for continuous adjustment of the laser energy from 0.1 to 5 μJ. The radiation was coupled into the scheme of a Michelson interferometer with a beam splitter 2 and directed in equal proportions in the pump and probe channels. Radiation in the probe channel was weakened by neutral filter 3. The probe and pump pulses with orthogonal polarizations were tightly focused by the Philips CAY033 lens in the scope of crystalline dielectric (LiF, CaF_2, BaF_2) 8. The probe pulse and its third harmonic were extracted from the pump pulse by Glan prism 1. The energies of the incident radiation and the probe pulse transmitted through the sample were simultaneously measured by Ge photodetector 4. The third harmonic energy of the probe pulse transmitted through band-pass filter ($\lambda = 410 \pm 5$ nm) 5 was registered by photomultiplier 6. The energies of the pump and probe pulses were selected, respectively, above and below the plasma formation threshold in the crystalline dielectric. After each laser pulse the sample was displaced in two directions by motorized translators in the perpendicular plane with a step of 20 μm. The delay time between the pump and probe pulses was varied in the probe channel of the Michelson interferometer by a motorized mirror positioning stage with a step of 2.5 μm (corresponding to a time step of 8.3 fs).

3. Results

All the crystals presented in this letter have the symmetry group $Fm\bar{3}m$ and have the O_h type of symmetry. With this type of crystal symmetry normal vibrations with symmetries of $A_{1g}, A_{1u}, A_{2g}, A_{2u}, E_u, E_g, T_u, T_g, T_{2u}$ and T_{2g} are possible [33]. The coherent phonon generation occurs in the Raman active modes. For these types of crystals, there are some Raman active modes with symmetries A_{1g}, E_g and T_{2g}. Thus, for the A_{1g} vibrations the Raman tensor is completely symmetric, for the E_g vibrations it is doubly degenerate and for the T_{2g} vibrations it is triply degenerate [33]. The corresponding tensors are given in table 1.

To determine the plasma formation threshold in fluorine-containing crystals the fundamental and the third harmonic radiation energies transmitted through the sample as a function of laser energy were registered (see figure 3). In the time-resolved experiments the pump and probe pulse energies were chosen above and below the plasma formation threshold respectively. The results for the samples are as follows: in BaF_2 crystal $E1 = 1$ μJ and $E2 = 1.1$ μJ (figure 2(a)), in CaF_2 crystal $E1 = 0.8$ μJ and $E2 = 1.1$ μJ (figure 3(b)), in LiF crystal $E1 = 2.5$ and $E2 = 3.5$ μJ (figure 3(c)).

To study the processes of energy transfer from the laser-induced plasma to the phonon subsystem we carried out the experiments at different energies of the pump pulse. The transmittance and the third harmonic signal of the probe pulse as a function of the time delay relative to the pump pulse were registered (figure 4). Inasmuch as the third harmonic signal is more sensitive to the medium properties, the plot of the transmitted signal is not given.

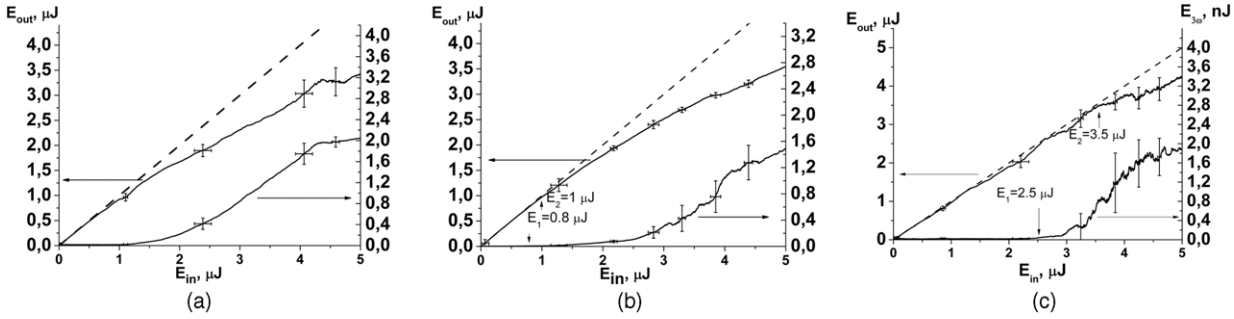

Figure 3. The transmitted laser pulse energy E_{out} and the third harmonic energy $E_{3\omega}$ as a function of laser pulse energy E_{in} in crystals of (a) BaF_2, (b) CaF_2 and (c) LiF. The dashed line represents the absence of absorption.

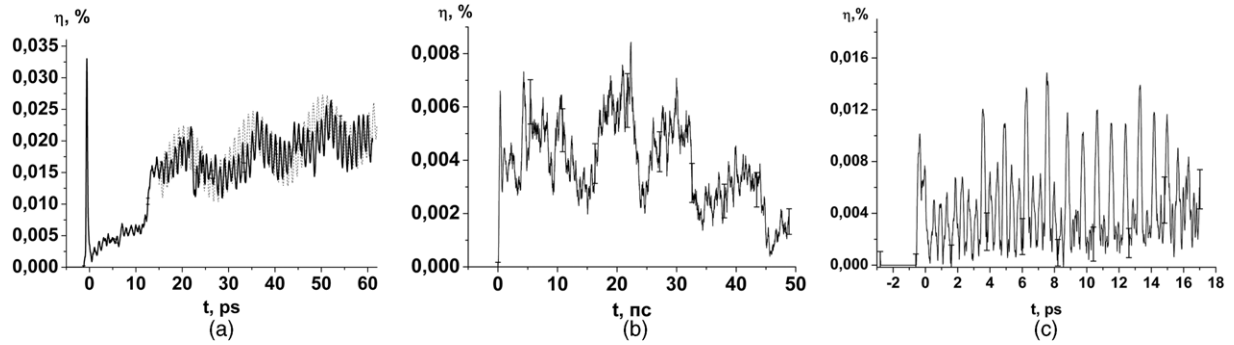

Figure 4. The THG efficiency η of the probe pulse in crystals of (a) BaF_2 at a pump pulse energy of 2 μJ, (b) CaF_2 at a pump pulse energy of 4 μJ and (c) LiF at a pump pulse energy of 3.6 μJ as a function of the time delay between the probe and pump pulses.

3.1. BaF_2 crystal

In the third harmonic signal of the probe pulse, coherent oscillations of different phonon modes were observed. Spectral analysis of the third harmonic probe pulse signal confirmed the presence of two quasiharmonic components in the signal with constant frequencies of 1 THz and ~67 GHz (the spectral error is about 20 GHz) (figure 5), corresponding to the Raman shifts of 33 cm^{-1} and 2.1 cm^{-1} observed in BaF_2 crystal in [34, 35] respectively. The lack of the T_{2g} mode at a frequency of 241 cm^{-1} [36] is related to the orientation of the crystal. The driving force is given by $F = (\Sigma_{uv}\chi^R_{uv}E_uE_v)$, where the E_u are the components of the optical pumping, $\chi^R_{uv} \approx \frac{\partial\chi_{uv}}{\partial Q}$ is the nonlinear Raman and χ_{uv} is the linear susceptibility [23], but the Raman tensor has only two non-zero components, namely, there are some directions for which the sum $\Sigma_{uv}\chi^R_{uv}E_uE_v$ vanishes. Then the integral $\int_{-\infty}^{t}\frac{\sin[\Omega(t-\tau)]}{\Omega}F(r,\tau)\mathrm{d}\tau$ (r is the vector of spatial coordinates, t is the time coordinate) goes to zero and there are no oscillations $Q(\boldsymbol{r}, t) = \int_{-\infty}^{t}\frac{\sin[\Omega(t-\tau)]}{\Omega}F(\boldsymbol{r},\tau)\mathrm{d}\tau$.

At lower energies of the pump pulse (1.4 μJ) only a high-frequency phonon mode at 1 THz was observed. This component is likely associated with A_{1g} symmetry oscillations which were observed at similar frequencies in other crystals belonging to the group symmetry of O_h [37]. A significant increase in the third harmonic signal amplitude of the probe pulse for values of the time delay longer than 15 ps was revealed. This means that coherent phonons are not immediately excited with the pump pulse arrival, but with a delay associated with the energy transfer from the plasma electrons to the phonon subsystem (figure 5). This delay explained using the theory of deformation potential. In this theory, the transport relaxation time τ_k characterizes the energy transfer from the plasma electrons to acoustic phonons. In the simplest case, it is estimated by $\frac{1}{\tau_k} \approx \frac{|\xi|^2 m_c\theta k}{\pi\rho c_s^2\hbar^3}$, where ξ is the deformation potential constant, m_c is the the effective mass of the electron, $\theta = k_bT$ (T is the temperature of the crystal lattice, k_b is the Boltzmann constant), k is the wavevector of the electrons in the plasma, ρ is the barium fluoride crystal

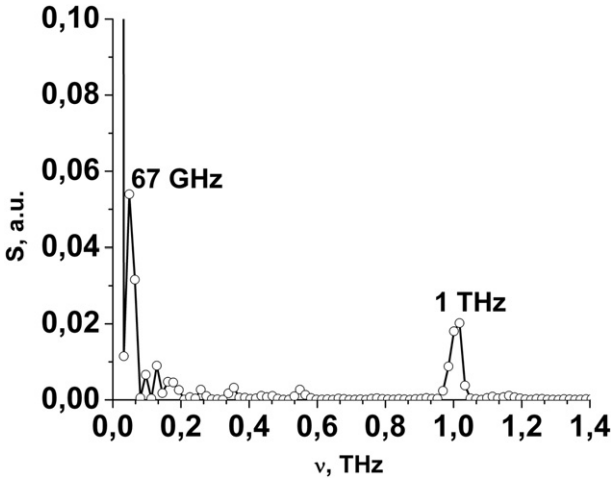

Figure 5. The spectral power density of the THG, S (ν), as a function of frequency in BaF_2 crystal at a pump pulse energy of 2 μJ.

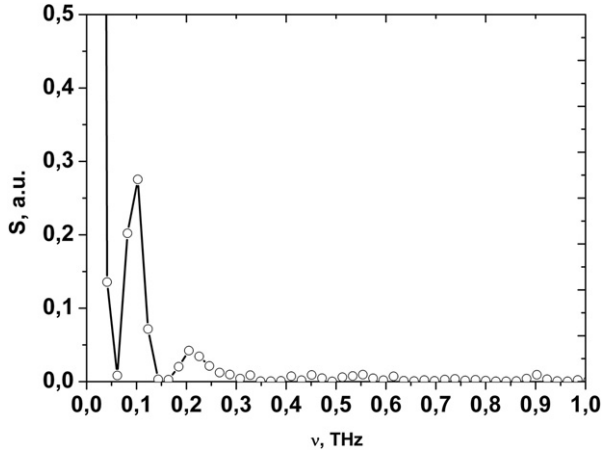

Figure 6. Spectral power density S (ν) of the probe pulse third harmonic signal in the CaF_2 crystal.

density and c_s is the speed of sound in the medium [38]. For this estimate, the following parameters were used: $|\xi| \approx 8$ eV which is the order of the electron energy in the outer nuclear membrane, $m_c \sim 0,5m_0$, where m_0 is the electron mass, $T \approx 300$ K, $\rho \approx 4,8$ g cm^{-3}, $c_s \approx 4.29$ km s^{-1}, the wavevector of the electrons was estimated from the kinetic energy of the order of 4 eV. With these parameters, the transport time is set to 13 ps.

3.2. CaF_2 crystal

In the CaF_2 crystal, behavior similar to the barium fluoride crystal was observed. In the CaF_2 crystal, in the third harmonic signal low-frequency oscillations with a frequency of 100 ± 20 GHz (figure 6) corresponding to a Raman shift of 3 cm^{-1} typical for acoustic phonons were also present [35].

On the background of low-frequency oscillations the third harmonic signal of the probe pulse contained high-frequency oscillations on different frequencies. Signal filtering of the third harmonic of the probe pulse in the frequency range from 0.8 to 1.2 THz could distinguish a low-intensity spectral component with a frequency of ∼1 THz. Oscillations in the frequency corresponding to the Raman shift of 322 cm^{-1} typical for T_{2g} oscillations were not observed during the experiment, due to the crystal's orientation in space.

3.3. LiF crystal

In LiF crystal, in the third harmonic of the probe pulse signal the coherent oscillations of different phonon modes were observed. Spectral analysis of the data has shown that the microplasma formed in a bulk of LiF crystal leads to excitation of several phonon waves, which are the overtones of the fundamental frequency of 0.38 THz [9] (figure 7).

In addition, energy transfer from one phonon mode to another was registered. This is possible only under strong excitation, when the ions are in inharmonic motion [39]. For instance, at the time interval up to 9 ps there are several phonon waves—the fundamental ($\omega = 0.38$ THz) and the overtone at 2ω with a modulation of 6ω. However, starting with a time delay of 9 ps, phonon waves with frequencies $\omega, 2\omega$ and 6ω disappear and the overtone of 3ω with a frequency of 1.14 THz appears. Inharmonic lattice excitation of LiF occurs because of the strong energy deposition in the laser-induced plasma relaxation process.

4. Conclusion

In this letter, the excitation and relaxation dynamics of coherent phonons in fluorine-containing crystals were investigated. For the first time, in the recorded signals of the third harmonic generated by the probe pulse in BaF_2 and CaF_2 crystals delays caused by a significant increase in phonon wave amplitude were observed. These delays are related to the time of energy transfer from the electronic to the phonon subsystem. In the LiF crystal energy transfer between many phonon modes was observed, which is possibly related to the anharmonicity of the phonon waves. It is important to note that the significant difference between experiments on the excitation of coherent phonons and canonical work [23, 37]

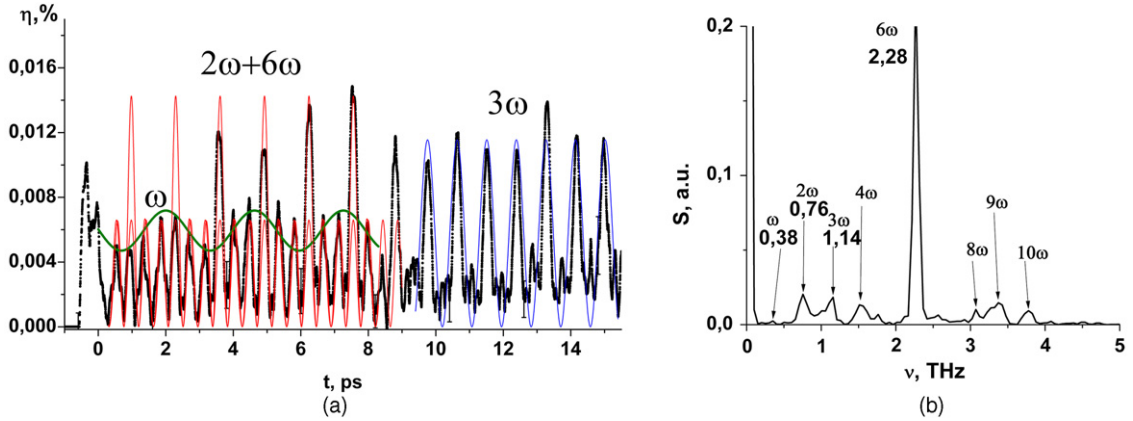

Figure 7. (a) Figure 4(c) with the phonon modes. (b) The power spectral density $S(\nu)$ of the probe pulse third harmonic signal in the LiF crystal.

described in this letter is due to the presence of laser-induced plasma as the effective energy transfer channel. In this letter it was shown that the laser-induced microplasma formed in a bulk of a crystalline dielectric plays a significant role in coherent phonon excitation and relaxation dynamics.

References

[1] Sibbett W, Lagatsky A A and Brown C T A 2012 The development and application of femtosecond laser systems *Opt. Express* **20** 6989–7001

[2] Dausinger F, Lichtner F and Lubatchowski H (ed) 2004 *Femtosecond Technology for Technical and Medical Applications* (*Topics in Applied Physics* vol 96) (Berlin: Springer)

[3] Sobol E *et al* 2000 Laser reshaping of cartilage *Biotechnol. Genet. Eng. Rev.* **17** 553–78

[4] Fankhauser F and Kwasniewska S 2003 *Lasers in Ophthalmology Basic, Diagnostics and Surgical Aspects* (The Netherlands: Kugler) pp 415–27

[5] Lu Y and Chen S C 2004 Micro and nano-fabrication of biodegradable polymers for drug delivery *Adv. Drug Deliv. Rev.* **56** 1621–33

[6] Ovsianikov A, Ostendorf A and Chichkov B N 2007 Three-dimensional photofabrication with femtosecond lasers for applications in photonics and biomedicine *Appl. Surf. Sci.* **253** 6599–602

[7] Miwa M, Juodkazis S, Kawakami T, Matsuo S and Misawa H 2001 Femtosecond two-photon stereo-lithography *Appl. Phys.* A **73** 561–6

[8] Kling M F and Vrakking M J J 2008 Attosecond electron dynamics *Annu. Rev. Phys. Chem.* **59** 463–92

[9] Gattass R R and Mazur E 2008 Femtosecond laser micromachining in transparent materials *Nature Photon.* **2** 219–25

[10] Ueki H, Kawata Y and Kawata S 1996 Three-dimensional optical bit-memory recording and reading with a photorefractive crystal: analysis and experiment *Appl. Opt.* **35** 2457–65

[11] Santos A D *et al* 1994 Space–time observation of an electron gas in SiO_2 *Phys. Rev. Lett.* **73** 1990–3

[12] Burenkov I A, Popov A M, Tikhonova O V and Volkova E A 2010 New features of interaction of atomic and molecular systems with intense ultrashort laser pulses *Laser Phys. Lett.* **7** 409–34

[13] Varró S, Gál K and Földes I B 2004 Intensity dependent anomalous transmittivity of thin plasma layers *Laser Phys. Lett.* **1** 111–4

[14] Sun Q, Jiang H, Liu Y, Wu Z, Yang H and Gong Q 2006 Diagnose parameters of plasma induced by femtosecond laser pulse in quartz and glasses *Front. Phys. China* **1** 67–71

[15] Cho S, Kumagai H and Midorikawa K 2002 *In situ* observation of dynamics of plasma formation and refractive index modification in silica glasses excited by a femtosecond laser *Opt. Commun.* **207** 243–53

[16] Nelson K A, Weiner A M, Leaird D E and Wiederrecht G P 1990 Femtosecond pulse sequences used for optical manipulation of molecular motion *Science* **247** 1317–9

[17] Bunkin A F, Pershin S M and Nurmatov A A 2006 Four-photon laser spectroscopy of solids in 0–0.15 THz *Laser Phys. Lett.* **3** 181–4

[18] Bartels R A, Backus S, Murnane M M and Kapteyn H C 2003 Impulsive stimulated Raman scattering of molecular vibrations using nonlinear pulse shaping *Chem. Phys. Lett.* **374** 326–33

[19] Hellwarth R W 1963 Theory of stimulated Raman scattering *Phys. Rev.* **130** 1850–2

[20] Carman R L, Shimizu F, Wang C S and Bloembergen N 1970 Theory of Stokes pulse shapes in transient stimulated Raman scattering *Phys. Rev.* A **2** 60–72

[21] Ruhman S, Joly A G and Nelson K A 1988 Coherent molecular vibrational motion observed in the time domain through impulsive stimulated Raman scattering *J. Quantum Electron.* **24** 460–9

[22] Yan Y, Gamble E B and Nelson K A 1985 Impulsive stimulated scattering: general importance in femtosecond laser pulse interactions with matter, and spectroscopic applications *J. Chem. Phys.* **83** 5391–9

[23] Merlin R 1997 Generating coherent THz phonons with light pulses *Solid State Commun.* **102** 207–20

[24] Zeiger H, Cheng T, Ippen E, Vidal J, Dresselhaus G and Dresselhaus M 1996 Femtosecond studies of the phase transition in Ti_2O_3 *Phys. Rev.* B **54** 105–23

[25] Stevens T E, Kuhl J and Merlin R 2002 Coherent phonon generation and the two stimulated Raman tensors *Phys. Rev.* B **65** 3–6

[26] Gordienko V M, Mikheev P M and Potemkin F V 2010 Generation of coherent terahertz phonons by sharp focusing of a femtosecond laser beam in the bulk of crystalline insulators in a regime of plasma formation *JETP Lett.* **92** 502–6

[27] Mikheev P M and Potemkin F V 2011 Generation of the third harmonic of near IR femtosecond laser radiation tightly focused into the bulk of a transparent dielectric in the regime of plasma formation *Moscow Univ. Phys. Bull.* **66** 19–24

[28] Gordienko V M, Potemkin F V and Mikheev P M 2009 Evolution of a femtosecond laser-induced plasma and energy transfer processes in a SiO_2 microvolume detected by the third harmonic generation technique *JETP Lett.* **90** 263–7

[29] Gordienko V M, Khodakovskij N G, Mikheev P M and Potemkin F V 2009 THG in dielectrics using low-energy tightly-focused IR femtosecond laser: third-order nonlinearity measurements and the evolution of laser-induced plasma *J. Russ. Laser Res.* **30** 599–608

[30] Potemkin F V and Mikheev P M 2012 Efficient generation of coherent THz phonons with a strong change in frequency excited by femtosecond laser plasma formed in a bulk of quartz *Eur. Phys. J.* D **66** 248–53

[31] Cheng T K, Acioli L H, Vidal J, Zeiger H J, Dresselhaus G, Dresselhaus M S and Ippen E P 1993 Modulation of a semicondutor-to-semimetal transition at 7 THz via coherent lattice vibrations *Appl. Phys. Lett.* **62** 1901–3

[32] Konorov S O *et al* 2004 Generation of the second and third harmonics of femtosecond Cr: forsterite laser pulses in SiC/PMMA nanopowder films *Laser Phys. Lett.* **1** 37–41

[33] Herzberg G 1963 *Molecular Specta and Molecular Structure* (Princeton, NJ: D van Nostrand)

[34] Kadlec F, Simon P and Raimboux N 1999 Vibrational spectra of superionic crystals $(BaF_2)_{1-x}(LaF_3)_x$ *J. Phys. Chem. Solids* **60** 861–6

[35] Taylor P and Loudon R 2006 The Raman effect in crystals *Adv. Phys.* 424–73

[36] Tu J and Sievers A 2002 Experimental study of Raman-active two-level systems and the boson peak in LaF_3-doped fluorite mixed crystals *Phys. Rev.* B **66** 1–16

[37] Garrett G A, Albrecht T F, Whitaker J F and Merlin R 1970 Coherent THz phonons driven by light pulses and the Sb problem: what is the mechanism? *Phys. Rev. Lett.* **77** 3661–4

[38] Harrison W 1970 *Solid State Theory* (New York: McGraw-Hill) pp 365–421

[39] Dove M 1993 *Introduction to Lattice Dynamics* (Cambridge: Cambridge University Press) pp 101–32